International Journal of Research
Available at https://edupediapublications.org/journals
e-ISSN: 2348-6848
p-ISSN: 2348-795X
Volume 04 Issue 14
November 2017

Active and Reactive Power Control During Unbalanced Grid Voltage in PV systems

[1]**Mr.Ramu Joga**, M.Tech, ramuujoga@gmail.com **Asst. Professor,**

[2]**Mr.YAnjaiah**, **Assistant Professor,**

[1,2]EEE Department,SWATHI INSTITUTE OF TECHNOLOGY AND SCIENCES,
Blatasingaram, Hayat Nagar, Rangareddy District, Hyderabad, Telangana-500075

***Abstract* — This paper presents a control strategy for a grid connected photovoltaic (PV) system aiming to regulate the active and reactive power injected to the electric system during asymmetrical voltage faults. The active power reference is obtained from a Maximum Power Point Tracking (MPPT) algorithm. The proposed control strategy generates the required reference currents to be imposed by the grid-tied inverter from the desired active and reactive power and the measured supply voltage. The scheme is validated for a single stage PV system where the inverter currents are regulated via predictive control. Results showing the performance of the strategy are presented during unbalanced voltage sags and swells.**

Keywords—Solar power generation, MPPT, Current control, Power generation control, Voltage unbalance, Low-voltage ride through (LVRT)

I. INTRODUCTION

Nowadays, grid-connected photovoltaic systems have become one of the fastest growing and most promising renewable energy sources in the world. In 2018 it is estimated a worldwide PV installed power of about 321 GW, in the most conservative scenario, that is twice the installed power in 2013 [1].

Grid-connected photovoltaic systems must convert the DC electrical energy generated by solar irradiation into AC electrical energy. The grid connected PV energy conversion systems can be grouped in two types: 1) Single stage: with only one power converter which handles all tasks, i.e. maximum power point tracking (MPPT) and grid current control, 2) Multi stage: where the addition of one or more DC/DC converters is used to carry out MPPT. However, multi stage systems have some drawbacks such as a lower efficiency and reliability, higher cost, and larger size in comparison to single stage systems [2], [3].

Different current controllers have been suggested in the literature to inject the desired active and reactive power during a voltage unbalance. In [4]-[5] a review for four scalar control schemes is presented for failures without zero sequence voltage. The general principle of the aforementioned methods is to measure the three-phase grid voltage and decompose it in positive and negative sequence; then the control strategy uses one or both sequence components to calculate the current reference during a voltage fault: (1) Instantaneous active reactive control (IARC) generates active/reactive power constant during grid fault but with a high level of THD(i) and unbalanced currents, (2) positive-negative sequence control (PNSC) generates active power with a ripple, reactive power constant, null THDi and unbalanced currents, (3) average active reactive control (AARC) generates reactive power with a ripple, active power constant, null THDi and unbalanced currents and (4) balanced positive sequence control (BPSC) generates active/reactive power with a ripple, null THDi and balanced currents. Based on the control schemes mentioned above a Flexible Voltage Support Control is proposed in [6] that allows choosing between active/reactive ripple and THD current in the system. In [7] a comparison between Synchronous Reference Frame Control (Syn-RFC, dq) and Stationary reference frame control with a Resonant Controller (St-RFC, αβ) is carried out, where it is concluded that both control strategies maintain the desired active/reactive power during grid fault but presenting the St-RFC better dynamic behaviour. In [8] the performance of a Grid Connected PV system is evaluated with a droop control for Low Voltage Ride through (LVRT) requirements and a PI controller with a Moving Average Filter is included in the control loop to reduce the ripple in the current references from the voltage in the DC link, obtaining an active/reactive power less than desired but with a lower ripple.

This paper presents a control strategy for single stage PV systems designed to inject the desired active and reactive power during unbalanced voltage sags and swells, including a strategy for the accurate control of currents. Voltage faults containing negative, positive and zero sequence voltages are considered. Voltage faults containing zero sequence voltage is an issue not addressed in previous works on this subject. The proposal strategy is validating for an 186kW photovoltaic plant using Matlab/Simulink. The scheme for the PV plant is a single-stage where a predictive grid-current control is applied. It is shown that the control scheme operated in normal and unbalanced conditions injecting the desired power references.

II. PHOTOVOLTAIC SYSTEM

A large PV plant with centralized configuration or string configuration presents the scheme shown in Fig. 1. The PV array is connected to the grid by a power converter which carries out MPPT as well as controls of the active and reactive power flow. Most PV systems operate below a thousand volts hence a transformer is used to increase the Low voltage (LV) generated to a Medium Voltage (MV); typically in star-delta connection (Y-Δ).The power from the PV plant is transmitted to a substation where a transformer elevates the voltages from medium to high voltage power transmission.

The grid-connected photovoltaic system is presented in Fig. 2, where the variables required to control the system are shown. The PV module array is connected to a single stage inverter which must ensure the injection of active power

calculated with some method to obtain MPPT. In this work the Perturb & Observe (P&O) method is used [9], [10].

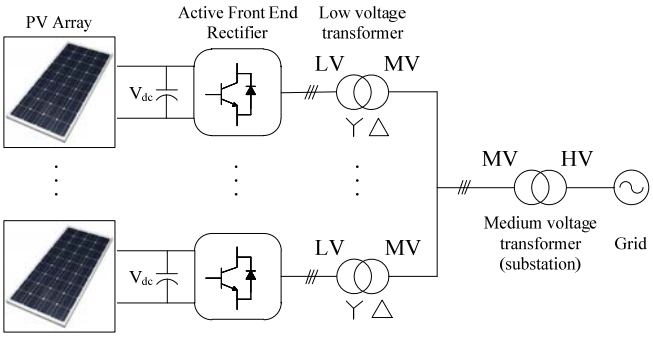

Fig. 1. Typical scale PV plant connected to the grid.

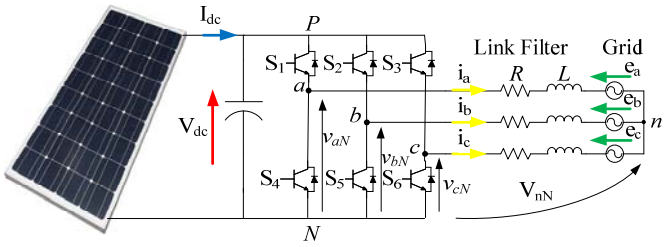

Fig. 2. Grid-connected photovoltaic system.

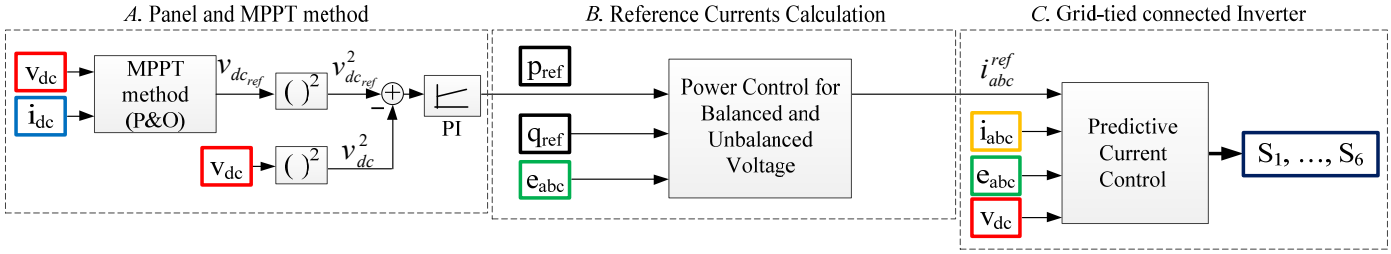

Fig. 3. Control Scheme for Grid-connected photovoltaic system for balanced and unbalanced grid voltage conditions.

Fig. 3 shows the control scheme for the grid-connected photovoltaic system. This control scheme can be separated in three stages: PV Panel and MPPT method, Reference Currents Calculation and Grid-tied connected inverter current control.

A. PV Panel and MPPT method

A commercial PV array is set with several photovoltaic cells connected in series or parallel, which define the maximum power voltage (VMPPT) and current (IMPPT), the short circuit current (ISC) and open circuit voltage (VOC). The parameters of commercial PV panel considered in this work, are shown in Table I for an irradiation of 1000 W/m2 and a temperature of 25°C, from the company Sunedison model D330. An array of 570 PV panels is considered. As previously mentioned, the single stage converter must perform the PV plant MPPT. In this work, a standard Perturb and Observe method (P&O) will be used [10].

The MPPT tracking scheme is done every 1s and a 5V voltage perturbation is used. Once the DC-link reference voltage is obtained, a PI controller is used [11] to control the DC voltage by setting the power injected to the grid. A scheme of the control loop is shown in Fig. 4 where h_{inv} is a model of the inverter and C is the DC link capacitor value.

TABLE I. PV PANEL PARAMETERS

P_{mppt}	325 W
I_{mppt}	8.69 A
V_{mppt}	37.4 V
I_{SC}	9.14 V
V_{OC}	46 V
Number of PV panels	570

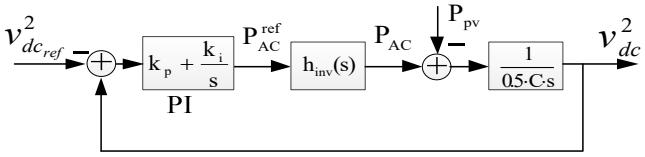

Fig. 4. DC link voltage control strategy.

B. Reference Current Calculation

The objective of the proposed strategy is to control the active and reactive power supplied to the grid by the power converter. The presented method assumes known instantaneous active/reactive power references and grid voltage [12].

Considering the grid voltage and current in abc coordinates $[v_{abc}] = [v_a \quad v_b \quad v_c]^t$ and $[i_{abc}] = [i_a \quad i_b \quad i_c]^t$, then the active power is obtained as $p(t) = [v_{abc}]^t \cdot [i_{abc}]$. Using Clarke's transformation, presented in (1) the instantaneous active power *p(t)* could be written in $\alpha\beta\gamma$ coordinates.

$$T_{abc\to\alpha\beta\gamma} = T = \frac{2}{3}\begin{bmatrix} 1 & -\frac{1}{2} & -\frac{1}{2} \\ 0 & \frac{\sqrt{3}}{2} & -\frac{\sqrt{3}}{2} \\ \frac{1}{2} & \frac{1}{2} & \frac{1}{2} \end{bmatrix} \quad (1)$$

Using $[v_{abc}] = T^{-1}[v_{\alpha\beta\gamma}]$ and $[i_{abc}] = T^{-1}[i_{\alpha\beta\gamma}]$, *p(t)* in $\alpha\beta\gamma$ coordinates is:

$$p(t) = \left(T^{-1}[v_{\alpha\beta\gamma}]\right)^t \cdot \left(T^{-1}[i_{\alpha\beta\gamma}]\right) \quad (2)$$

$$p(t) = [v_{\alpha\beta\gamma}]^t (T^{-1})^t \cdot (T^{-1})[i_{\alpha\beta\gamma}] \quad (3)$$

Since $i_a + i_b + i_c = 0$, $p(t)$ is:

$$p(t) = \frac{3}{2} v_\alpha i_\alpha + \frac{3}{2} v_\beta i_\beta \quad (4)$$

Because the zero sequence current is null, (4) is still valid to obtain $p(t)$ even under the existence of zero sequence voltages in fault conditions.

The instantaneous reactive power is obtained as: $|[q_{abc}]| = |[v_{abc}] \times [i_{abc}]|$ and using $[v_{abc}] = T^{-1}[v_{\alpha\beta\gamma}]$ and $[i_{abc}] = T^{-1}[i_{\alpha\beta\gamma}]$, yields to [12]:

$$|[q_{abc}]| = \left|\left(T^{-1}[v_{\alpha\beta\gamma}]\right) \times \left(T^{-1}[i_{\alpha\beta\gamma}]\right)\right| \quad (5)$$

that it can be rewritten as:

$$|[q_{abc}]| = |T^{-1}| |T^t[v_{\alpha\beta\gamma}] \times [i_{\alpha\beta\gamma}]| \quad (6)$$

Developing (6), $|[q_{abc}]|$ using voltage and current alpha-beta-gamma (with null zero sequence current component) is:

$$|[q_{abc}]| = \frac{3}{2}\sqrt{2v_\gamma^2\left(i_\alpha^2 + i_\beta^2\right) + \left(v_\alpha i_\beta - v_\beta i_\alpha\right)^2} \quad (7)$$

The reference currents to supply an active power $P = \frac{2}{3} p_{ref}$ and reactive power $Q = \frac{2}{3}|q_{ref}|$ to the system is obtained using (4), (7) as:

$$i_{\alpha 1}^*, i_{\alpha 2}^* = \frac{P v_\alpha \mp v_\beta \sqrt{\frac{-2P^2 v_\gamma^2 + Q^2(v_\alpha^2 + v_\beta^2)}{2v_\gamma^2 + v_\alpha^2 + v_\beta^2}}}{v_\alpha^2 + v_\beta^2} \quad (8)$$

$$i_{\beta 1}^*, i_{\beta 2}^* = \frac{P v_\beta \pm v_\alpha \sqrt{\frac{-2P^2 v_\gamma^2 + Q^2(v_\alpha^2 + v_\beta^2)}{2v_\gamma^2 + v_\alpha^2 + v_\beta^2}}}{v_\alpha^2 + v_\beta^2} \quad (9)$$

The reference currents given by (8) relates to lagging power factor and those from (9) corresponds to a leading power factor. Reference currents in (8)-(9) must comply with $\frac{-2P^2 v_\gamma^2 + Q^2 v_\alpha^2 + Q^2 v_\beta^2}{2v_\gamma^2 + v_\alpha^2 + v_\beta^2} \geq 0$.

In order o have realistic reference currents (without imaginary components), p_{ref} and q_{ref} should fulfil the following condition:

$$|q|_{ref} \geq \frac{\sqrt{2} v_\gamma}{\sqrt{v_\alpha^2 + v_\beta^2}} p_{ref} \quad (10)$$

It should be noted that unbalanced voltage failures produced between the inverter and the transformer low voltage side could generate zero sequence voltages, for instance in a single phase fault.

C. Grid-tied connected Inverter

Full details of the Grid-tied connected inverter, see Fig. 2, control can be found in [13]. An outer standard DC link voltage control is used and an inner predictive current control is applied [14], [15], [16].

III. Simulations Results

The proposed control strategy has been simulated in Matlab considering an 186kW PV plant (570 PV panels of 325W each). A sampling period of 56μs is considered as this corresponds to the maximum switching frequency of the inverter that will be used to obtain experimental results in a future work, using an PV emulator a low power inverter. The system parameters used in the simulation are depicted in Table II.

TABLE II. SET-UP SYSTEM PARAMETERS

R	1 [mΩ]
L	0.2 [mH]
C	2400 [μF]
V_{rms}	220 V
N_s panel	19
N_{pp} panel	30
T_s	56 [μs]
f	50 Hz

A. Panel and MPPT method

Simulations results for normal operation of the PV system, without voltage faults, are shown with irradiation and temperature profile illustrated in Fig. 5.

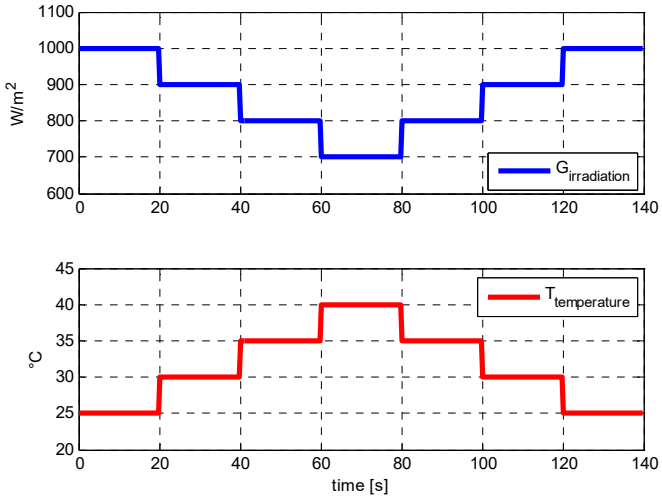

Fig. 5. Irradiation and Temperature Profile considered in the simulation results.

The reactive power injected to the grid is set to zero, unless otherwise stated, and the active power injected depends on the irradiation and panel temperature. The grid current, active power and reactive power are shown in Fig. 6. The active power changes from 185kW to 123.5kW, under MPPT conditions. The grid current changes from 480A to 325A.

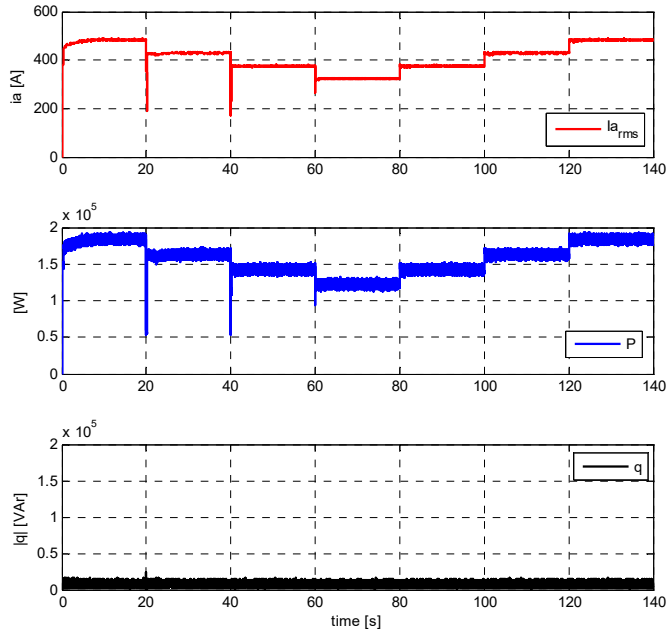

Fig. 6. Grid RMS Current, Active power and Reactive Power for normal operation.

Fig. 7 shows the current, voltage and power from the PV plant. The DC current changes from 260A to 181A. The DC initial voltage reference is set to 750V and fluctuates between 715V and 675V with a voltage ripple of 10V. The power delivered form the PV array is initially 175kW and then changes from 186kW to about 124kW. The difference in the active power between Fig. 6 and Fig.7 is due to system losses.

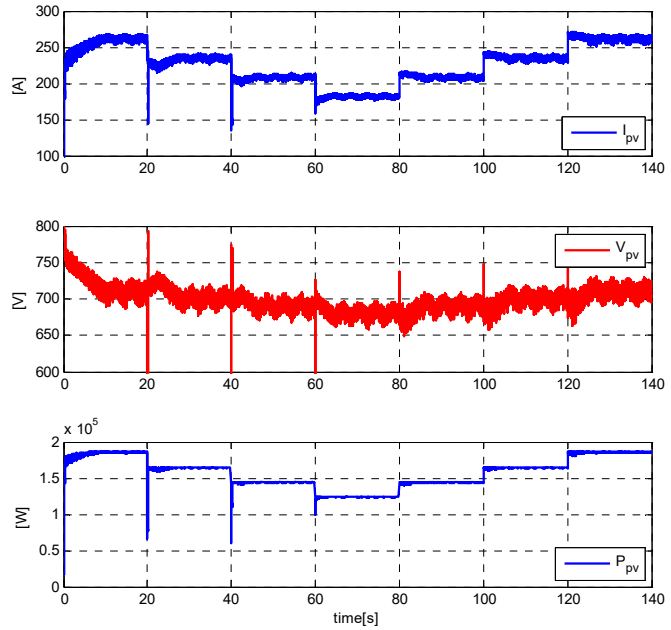

Fig. 7. Current, Voltage, Power for PV array.

B. Voltage Sag: 40% vb, 30% vc and 20% va

Three Voltage sag are applied in the system, see Fig. 8 (top). A 40% voltage reduction for phase B is applied during t=0.05s and t=0.2s, 30% voltage reduction in phase C is applied during t=0.1s and t=0.2s, and finally a 20% over voltage is caused in phase A from t=0.15(s) to t=0.2(s). The reference reactive power is set to zero, and the system is operating at MPPT with 1000W/m2 and 25°C generating 185kW. The current injected to the grid is shown in Fig. 8 (middle). The grid faults contain a zero sequence voltage and the restriction in (10) is not accomplished, hence the reactive current cannot be regulated during the faults. Before the fault the grid current is 486A. During the fault the PV plant keeps generating 185kW and the current reaches a maximum of 700A for the third fault. During the voltage sag the reactive power presents a ripple of 100Hz and reaches a maximum of 48kVAr .

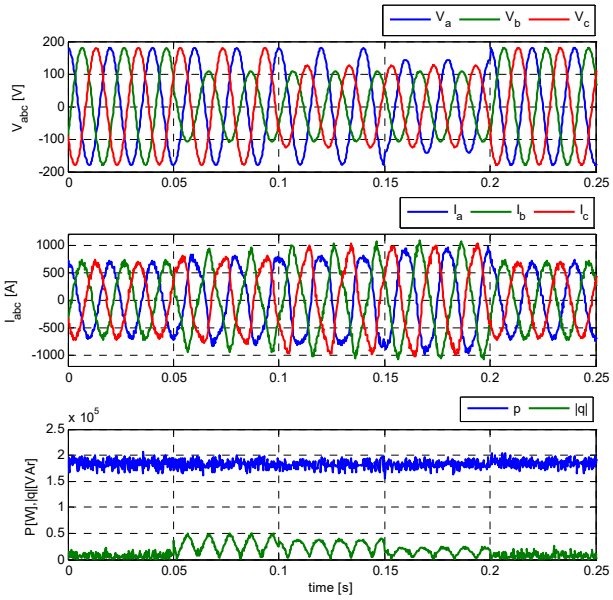

Fig. 8. Voltage (top), Grid Current (middle) and Active/Reactive Power injected (bottom) during a voltage sag.

Fig. 9 show simulation results when the reference reactive power is set 50kVAr for the same voltage sag conditions.

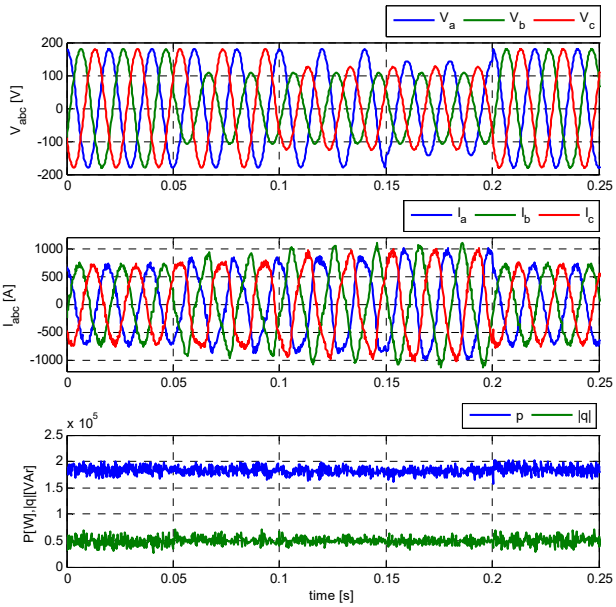

Fig. 9. Voltage (top), Grid Current (middle) and Active/Reactive Power.

Before the faults the grid current is 545(A). During the fault the grid current reached a peak value of 714A. The active/reactive powers during the grid faults are regulated in their references because the restriction in (10) is satisfied.

C. *Voltage Swell: 40% va, 30% vb and 20% vc*

Three Voltage swells are caused in the system, see Fig. 10 (top). A 40% voltage increase in phase B is applied during t=0.05s and 0.2s, a 30% voltage increase in phase C is applied during t=0.1s and t=0.2s, and finally a 20% voltage increase is caused in phase A from t=0.15s to t=0.2s. The reference reactive power is set to zero and the PV system is operating at MPPT for 1000W/m2 and 25°C. The current injected to the grid is shown in Fig. 10 (middle).

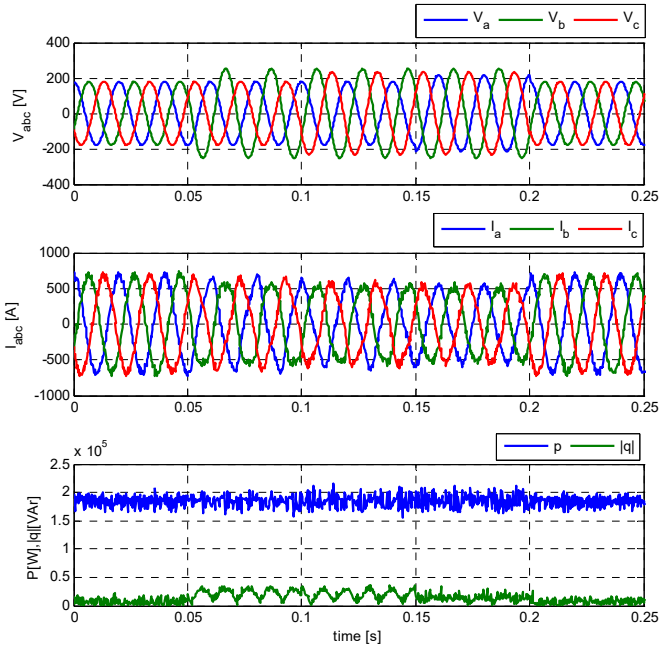

Fig. 10. Voltage, Current Grid and Active and Reactive Power injected during voltage swell.

The grid faults contain a zero sequence voltage and the restriction in (10) is not accomplished, therefore the reactive power cannot be regulated according to the reference value. Before the fault the grid current is 486A, and the PV plant is generating 185kW and the reactive power is null.

During the grid current reduces to 350A, the active power is maintained at the MPPT but the reactive power has a ripple of 100Hz. In order to satisfy (10), the reference reactive power is set to 32.5kVAr. The results are shown in Fig. 11.

The current before fault is 497A and the PV system generates 185kW. During the grid faults the active and reactive powers follow their corresponding references.

IV. Conclusion

This paper has shown a scheme to control the active power supplied for a photovoltaic power plant to a power supply system under grid faults conditions. The strategy is able to inject maximum power from the photovoltaic plant, for different solar radiation and temperature profiles, during grid voltage sags and swells. Simulations results have been shown considering a realistic 186kW plant consisting on 570 PV panels of 325W each. The simulation results have validated the proposed scheme. A low power experimental setup is being built to validate the strategy experimentally with a PV emulator.

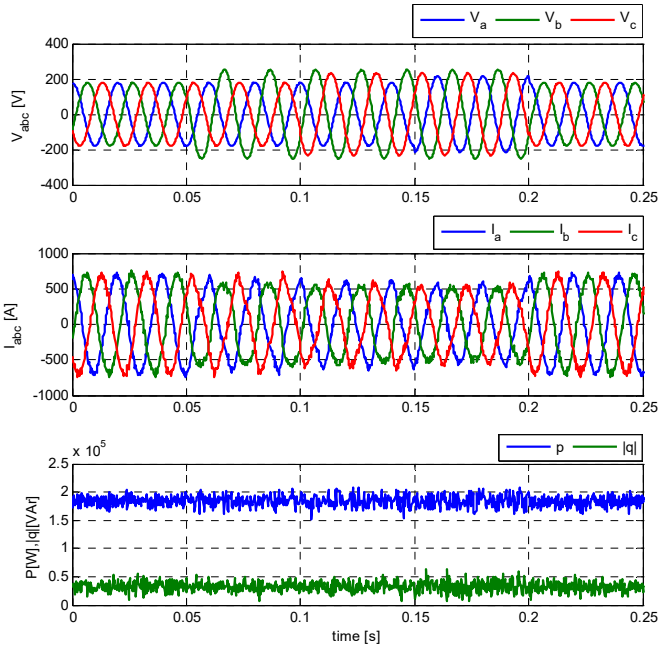

Fig. 11. Voltage, Current Grid and Active and Reactive Power injected during voltage swell.

References

[1] European Photovoltaic Industry Association. (2014). “Global market outlook for photovoltaics 2014-2018” . Available http://www.epia.org/fileadmin/user_upload/Publications/44_epia_gmo_report_ver_17_mr.pdf.

[2] G. M. Dousoky, E. M. Ahmed, and M. Shoyama, "MPPT Schemes for Single-Stage Three-Phase Grid-Connected Photovoltaic Voltage-Source Inverters", In Proc. IEEE-ICIT 2013, Feb. 2013, pp. 600-605.

[3] R. Mechouma, B. Azoui, and M. Chaabane, “Three-phase grid connected inverter for photovoltaic systems, a review,” in Proc. 1st Int. Conf. Renewable Energies Veh. Technol., 2012, pp. 37–42.

[4] M. Castilla, J. Miret, J. L. Sosa, J. Matas, and L. García de Vicuña, “Grid-fault control scheme for three-phase photovoltaic inverters with adjustable power quality characteristics,” IEEE Trans. Power Electron., vol. 25, no. 12, pp. 2930–2940, Dec. 2010.

[5] Teodorescu, R., Liserre, M., & Rodriguez, P. “Grid converters for photovoltaic and wind power systems”, Vol. 29. John Wiley & Sons. Inc, 2011

[6] A. Camacho, M. Castilla, J. Miret, J. Vasquez, and E. Alarcon-Gallo, “Flexible voltage support control for three-phase distributed generation inverters under grid fault,” IEEE Trans. Ind. Electron., vol. 60, no. 4, pp. 1429–1441, Apr. 2013.

[7] M. Diaz and R. Cardenas, "Analysis of synchronous and stationary reference frame control strategies to fulfill LVRT requirements in Wind Energy Conversion Systems, " in 2014 Ninth International Conference on Ecological Vehicles and Renewable Energies (EVER), 2014, pp. 1-8.

[8] M. Mirhosseini, J. Pou, and V. G. Agelidis, "Current improvement of a grid-connected photovoltaic system under unbalanced voltage conditions," in Proc. IEEE ECCE Asia Downunder (ECCE Asia), Jun. 2013, pp. 66–72.

[9] M.A. Elgendy, B. Zahawi and D. J. Atkinson, "Evaluation of P & O MPPT Algorithm Implementation Techniques," Sixth IET International Conference on Power Electronics, Machines and Drives, March 2012.

[10] Schmidt, H., Burger, B., Bussemas, U., & Elies, S. "How fast does an MPP tracker really need to be?". Proc. of 24th EuPVSEC, pp. 3273-3276. 2009

[11] Abu-Rub, Haitham, Mariusz Malinowski, and Kamal Al-Haddad. Power electronics for renewable energy systems, transportation and industrial applications. John Wiley & Sons, 2014.

[12] F.-Z. Peng and J.-S. Lai, "Generalized instantaneous reactive power theory for three-phase power systems," IEEE Trans. Instrum. Meas., vol. 45, no. 1, pp. 293–297, Feb. 1996.

[13] G. Hunter; R. Pena; I. Andrade; J. Riedemann; R. Blasco-Gimenez, "Power control of an AFE rectifier during unbalanced grid voltage using predictive current control", in Proc. IEEE 24th International Symposium on Industrial Electronics, 2015, Pages: 385 – 390.

[14] P. Cortes, J. Rodriguez, C. Silva, and A. Flores, "Delay compensation in model predictive current control of a three-phase inverter," IEEE Trans. Ind. Electron., vol. 59, no. 2, pp. 1323–1325, Feb. 2012.

[15] J. Rodríguez, J. Pontt, C. Silva, P. Correa, P. Lezana, P. Cortés, and U. Ammann, "Predictive current control of a voltage source inverter," IEEE Trans. Ind. Electron., vol. 54, no. 1, pp. 495–503, Feb. 2007.

[16] J. Rodriguez and P. Cortes, Predictive control of power converters and electrical drives, vol. 37. John Wiley & Sons, 2012.

Author Details:

Mr.Ramu Joga
Asst. Professor
M.Tech
email: ramuujoga@gmail.com
SWATHI INSTITUTE OF TECHNOLOGY AND SCIENCES,
Blatasingaram , Hayat Nagar , Rangareddy District , Hyderabad, Telangana-500075.